JOURNAL OF OPTOELECTRONICS AND ADVANCED MATERIALS Vol. 8, No. 2, April 2006, p. 604 - 610

Structural and morphological properties of perylene derivatives films on passivated semiconductor substrates

G. SALVAN[a*], S. SILAGHI[a], M. FRIEDRICH[a], C. HIMCINSCHI[a,b], D. R. T. ZAHN[a]
[a]*Institut für Physik, Technische Universität Chemnitz, 09107 Chemnitz, Germany*
[b]*present address: Max-Planck-Institut für Mikrostrukturphysik, Weinberg 2, D-06120 Halle, Germany*

Molecules of 3,4,9,10-perylene-tetracarboxylic dianhydride (PTCDA) and N,N'-dimethyl 3,4,9,10-perylene-tetracarboxylic diimide (DiMe-PTCDI) were deposited by organic molecular beam deposition onto passivated Si(100) and GaAs(100) substrates in ultra high vacuum. Raman spectroscopy was employed to investigate *in situ* the influence of the substrate temperature during film growth on the structural properties and the morphology of organic films. Infrared spectroscopy was used to extract information on the molecular orientation. The results are complemented by those obtained from topographic imaging techniques, such as scanning electron microscopy (SEM) and atomic force microscopy (AFM) results.

(Received January 18, 2006; accepted March 23, 2006)

Keywords: PTCDA, DiMe-PTCDI, GaAs(100), Si(100), Surface passivation, Raman spectroscopy, AFM, SEM

1. Introduction

Amongst the many-fold applications of organic thin films the use as active interlayers in metal/inorganic semiconductor junctions for the high-frequency and microwave technology appears to be very promising. Recently it was shown that the introduction of a perylene derivative 3,4,9,10-perylenetetracarboxylic dianhydride (PTCDA) as interlayer in hybrid Ag/PTCDA/InP [1] and Ag/PTCDA/GaAs [2] junctions allows bias voltages during operation to be lowered. An estimate of 42 GHz is given for the high frequency limit for an optimised InP based device [1] which is about one third of the frequency achievable by commercially available GaAs Schottky diodes. By introducing a thin organic molecular film between Ag and GaAs(100), the effective barrier height systematically varies depending on the PTCDA layer thickness and the GaAs(100) surface treatment [2]. Another important issue remains to be investigated, namely the influence of different organic interlayers on the device performance. A logic approach would be to consider molecules from the same class of perylene derivatives with different end-groups, e.g. replacing the oxygen atom of each anhydride group in PTCDA with a nitrogen atom connected to a methyl group yields the molecule of N,N'-dimethyl 3,4,9,10-perylene-tetracarboxylic diimide (DiMe-PTCDI).

The structural properties of PTCDA films grown at RT on selenium passivated GaAs(100) interfaces were assessed by means of low energy electron diffraction (LEED) and scanning tunnelling microscopy (STM) [3,4,5]. The strong interaction between PTCDA and semiconductor surfaces is considerably reduced by the passivation of the surface prior to the growth of the organic film [6,7]. Improved crystallinity is also observed for deposition onto sulphur passivated GaAs(100) [8,9]. The thin films of PTCDA were found to consist of two polymorphs labelled α and β [10,11]. Both crystallize in the space group $P2_1/c$ but have different lattice constants [12]. The unit cell contains 2 molecules which are arranged in a herringbone packing with the molecular planes parallel to the (102) lattice plane. In the α modification the overlap between molecules in adjacent (102) crystalline planes is reduced by shifting along the short unit cell axis, while the reduction for the β phase occurs via shifting along the long axis. Additionally, the area of the unit cell projected onto the (102) plane is lower in the α- compared to β- phase. DiMe-PTCDI crystallizes in the same monoclinic structure as PTCDA [13].

For organic materials relevant for organic light emitting diodes a better control over the device performance has been achieved by changing the morphology of the organic film by varying the substrate temperature during film growth [14,15]. In this paper the results of Raman spectroscopy are compared with AFM and SEM results for PTCDA/H-Si(100), PTCDA/S-GaAs(100), and DiMe-PTCDI/S-GaAs in order to obtain a comprehensive understanding on the structural and morphological properties of films grown at different temperatures. Additionally, the molecular orientation within the films is assessed by infrared spectroscopy.

2. Experiment

P-type silicon (B-doped, 3-6 Ω·cm) (100) oriented substrates were wet-chemically treated under atmospheric conditions. The first step consists in 2 min etching in hydrofluoric acid (HF, 40%) to remove the silicon oxide and the organic contaminants, and thereafter hydrogen-passivate the dangling bonds on the surface. Secondly, rinsing in a buffered solution ($HF + NH_4OH + NH_4F$, pH

8-9) reduces the density of steps formed during the first processing step. The substrates were then transferred into the ultra-high vacuum (UHV) system. Low energy electron diffraction (LEED) showed a sharp 1x1 diffraction pattern of the hydrogen-passivated Si(100) surface. Si-doped (N_d=1.8×10^{18} and 2.7×10^{18} cm^{-3}) GaAs(100) wafers provided by Freiberger Compound Materials were also used as substrates. In order to clean and passivate the surface, the GaAs substrates were wet-chemically treated under atmospheric conditions. They were first degreased of organic contaminants by successively dipping into acetone, ethanol and de-ionised water in an ultrasonic bath, for 5 min each. The etching in S_2Cl_2+CCl_4 solution (1:3) removes the oxides and chemically passivates the surface dangling bonds with sulphur atoms. The substrates are then rinsed in acetone, ethanol and de-ionised water. The sulphur atoms in excess and residual alcohol molecules sticking to the surface are removed by annealing at 620 K in the UHV chamber at a base pressure below 2×10^{-8} Pa. The sharp LEED pattern reveals a 2x1 reconstruction. By analogy to a recent model proposed for Se-passivated GaAs(100):2×1 surfaces [16] the treatment is proposed to lead to a gallium-sulphide like layer with the surface terminated by single S atoms [17].

PTCDA and DiMe-PTCDI molecules purchased from Lancaster Synthesis and Syntec GmbH were thermally evaporated in UHV onto freshly prepared 1×1 H-Si and 2×1 S-GaAs(100) substrates. The evaporation rates were 0.3 nm/min for PTCDA and 0.24 nm/min for DiMe-PTCDI as determined by a quartz microbalance and an external calibration by means of atomic force microscopy (AFM). PTCDA films with a nominal thickness of 40 nm were deposited onto substrates maintained at various temperatures: 230 K (for Si), 250 K (for GaAs), and 295 K, 360 K and 410 K (for both). DiMe-PTCDI films with the same nominal thickness were deposited onto GaAs maintained at RT and 360 K. The substrate temperature was derived from the experimentally determined Raman shift of the Si and GaAs LO phonons (2.2 cm^{-1}/ 100 K and 1.8 cm^{-1}/ 100 K, respectively [18]) which is linear in the relevant temperature range.

The UHV chamber is optically aligned with a Raman spectrometer, allowing *in situ* measurements to be performed. The Raman spectra were excited with the 2.54 eV line of an Ar^+ laser. The scattered light is collected by a Dilor XY 800 triple monochromator with a multichannel charge coupled device detector. The spectral resolution was ~ 3 cm^{-1}, unless otherwise stated, as determined from the full width at half maximum (FWHM) of the laser line. Typical values of the incident laser power were in the range from 50 mW to 100 mW below the damage threshold of the absorbing PTCDA and DiMe-PTCDI films (~ 100 kW/cm^2). The infrared spectra were recorded using a Fourier transform infrared (FTIR) spectrometer Bruker IFS 66. Reflectance measurements with s-polarised light at the angle of incidence 20° were performed in the spectral range from 700 cm^{-1} to 2000 cm^{-1} and rotating the GaAs(100) substrate stepwise by an angle γ around its normal. The spectral resolution was better than 2 cm^{-1}.

The SEM imaging was performed using a Philips SEM 515 set-up with the electrons impinging on the sample having a kinetic energy of 30 keV. Topographic imaging was possible for all organic films investigated, which is an indication for their high electric conductivity. However, in order to improve the contrast a thin platinum film (~ 5 nm) was deposited by Ar sputtering onto the 40 nm PTCDA film grown at RT and onto the 40 nm DiMe-PTCDI films. This was proven to preserve the morphology of the organic film. The AFM measurements on PTCDA/S-GaAs system were performed with an Autoprobe CP® Thermomicroscope operated in contact-mode with a typical force of 2 nN.

3. Results and discussion

3.1. PTCDA/H-Si(100)

3.1.1. SEM

The PTCDA evaporation rate used in the present experiments leads to film growth only when the substrate temperature is below 470 K. The film colour varied from bluish green for the sample grown at 230 K to reddish brown for that at 410 K. SEM topographic images show that the films grown at RT (Fig. 1(a)) have a granular structure with average grain size of ~ 80-90 nm. The domain shape is preserved when grown on substrates kept at 360 K, but the average grain size is larger: ~ 200 nm (Fig. 1 (b)). Even larger domains are obtained when the growth takes place at 410 K (Fig. 1 (c)), but a large number of domains have needle-like shapes. In PTCDA films grown on KCl(100) substrates at 453 K the coexistence of such narrow needle-like crystallites with wider, plate-like and less regularly shaped domains was also observed [19]. The needle-like domains turned out to be α- modification whereas the laterally extended ones consist of β- modification [19]. From the SEM images in Fig. 1 it thus results that in the films grown on H-Si(100) substrates kept at 410 K the two polymorphs of PTCDA coexist, with a larger amount of molecules aggregating in α- phase. Since the shape of grains obtained at lower substrate temperatures is more uniform, an analysis of SEM images alone cannot provide information regarding the crystalline phases.

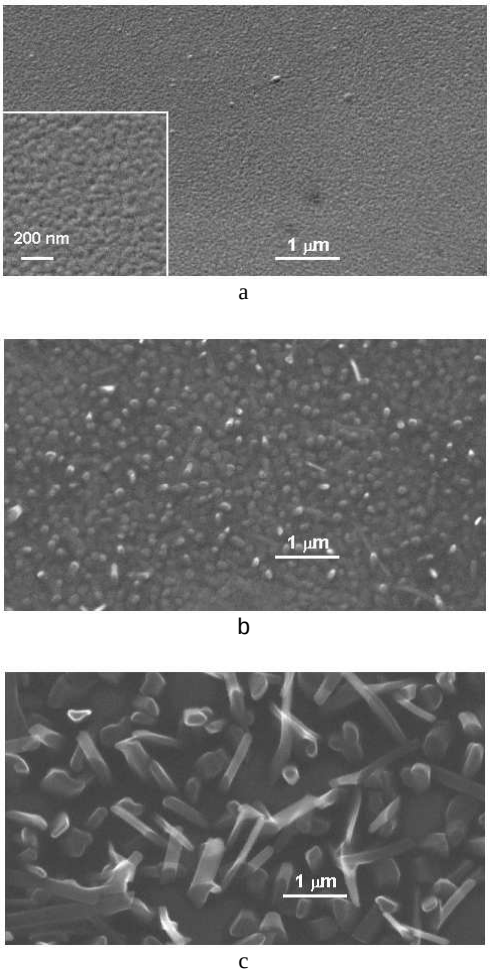

Fig. 1. SEM topographic images of PTCDA films grown on H-Si(100) substrates kept at RT (a), 360 K (b) and 410 K (c). The inset in (a) shows a higher magnification image.

3.1.2. Raman spectroscopy

Raman spectra of the films grown H-Si(100) substrates at various temperatures were recorded at RT and are displayed in Fig. 2. A normalization was performed with respect to the mode at 1303 cm^{-1} for a better comparison of relative intensities and of the background.

One marked feature is the presence of the phonon bands below 125 cm^{-1} associated with the crystalline nature of the films. Their intensity was enlarged several times for a better visualization. The frequency positions of bands observed for films correspond well to those of A_g and B_g phonons observed in the single crystal, but the change in the relative intensities with changing the polarization configuration is absent. This behaviour reflects the polycrystalline nature of films, with the crystalline domains having several preferred azimuthal orientations or being randomly oriented with respect to the substrate [20]. The increase of growth temperature is accompanied by a decrease of the FWHM of the phonon modes (Fig. 2). In [20] it was proposed that the correlation between the FWHM of phonon bands and the structural order is similar to that observed in the case of inorganic semiconductor systems, such as gallium arsenide [21] or germanium [22]. There, the decrease in the FWHM of the optical phonon bands is related to structural improvement induced by the growth or annealing temperature, i.e. to the development of larger and more perfect single crystalline domains at the expense of the amorphous and polycrystalline contributions.

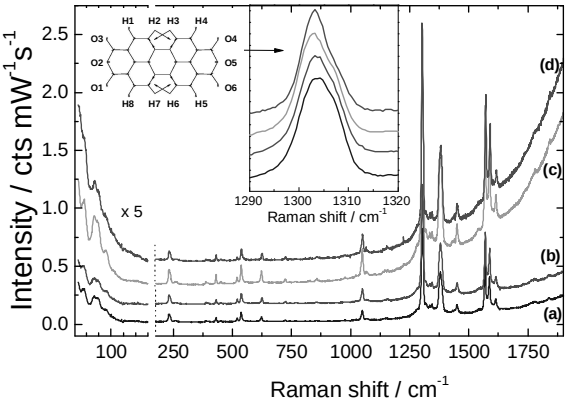

Fig. 2. Raman spectra of PTCDA films grown on H-Si(100) at four substrate temperatures: 230 K (a), 295 K (b), 360 K (c) and 410 K (d). The inset shows a zoom in the region of the most intense C-H mode.

Considering the most prominent internal mode at 1303 cm^{-1} (Fig. 4, inset), its FWHM decreases from (11±0.4) cm^{-1} to (8.8±0.4) cm^{-1}, for the samples grown at temperatures between 230 K and 410 K, respectively. This total decrease in FWHM may be an indication of improved crystallinity. The line narrowing, however, is accompanied by the occurrence of a pronounced asymmetry with increasing temperature. A multi-Lorentzian fitting procedure performed in the spectral range of 1185-1500 cm^{-1} reveals that the band at 1303 cm^{-1} consists of two components centred at (1302.9±0.2) cm^{-1} and (1306.7±0.2) cm^{-1}. The splitting between these components amounts to 3.8 cm^{-1} [20], whereas the Davydov splitting (1300.6 cm^{-1} - 1302.3 cm^{-1}) experimentally determined for a α- PTCDA crystal is 1.7 cm^{-1} [24]. Raman data for β-PTCDA single crystals were not reported up to date.

A first explanation for the origin of the two components would be the Davydov splitting [24]. However, the difference in the frequency and splitting values between spectra of films and α-phase crystals accounts for an overlapping of the splitting due to the coexistence of α- and β-PTCDA phases and the Davydov splitting for each phase [16]. In ref. [23] it was shown that the C-H band at 1303 cm^{-1} is the most susceptible among the bands detected under resonant conditions to suffer changes when the molecular environment changes. Considering the molecule in the centre of the unit cell two

of its H atoms (labelled with H2 and H6 in Fig. 4) are likely to be involved in H bridges [24]. These atoms belong to the group of four H atoms with the largest elongation during the vibration at 1303 cm^{-1} (Fig. 4). α- and β- phases are characterized by different molecular packing in the (102) plane (see Table 1) which leads to different strengths of H bridges and hence to different downward shifts of the C-H mode frequency [25] compared to the free molecule. The largest amount of shift to lower frequency compared to the free molecule should appear in the α- phase which has the closest packing and in which the H bridges are stronger. Thus the frequency of the C-H band of the molecules in α- phase should be lower than the frequency of the molecules in β- phase.

The background in the low and high frequency range of the Raman spectra (i.e. below 125 cm^{-1} and above 1600 cm^{-1}) is different for the samples grown at different temperatures. The polycrystalline nature of the films gives rise to surface roughness within the area of the laser beam focus (~ $6 \cdot 10^4$ μm^2). An increase in the size of the individual crystals with the substrate temperature is manifested macroscopically as an increase in the degree of roughness. As a consequence, the part of the light that is diffusely elastically scattered increases giving rise to the increasing background in the low wavenumber region.

Responsible for the background in the high frequency region is a photoluminescence (PL) process. The PTCDA films show a broad asymmetric PL band (~ 200 meV), with a maximum at about 1.75 eV when measured at RT [26]. For the samples grown at elevated temperatures a red shift is observed [26]. This behaviour, previously reported by Leonardth *et al.* [27], originates from the coexistence of α- and β- crystalline phases within the films. The shift follows the evolution of α- at the expense of β-phase with increasing substrate temperature, already evidenced by means of Raman spectroscopy and XRD. A limiting factor for the PL intensity resides in non-radiative processes. The non-radiative centres can be states located either at the silicon interface or at PTCDA domain surfaces or structural defects and impurities within the PTCDA domains. The increase in size of crystalline domains and the improved crystallinity reduces the defect density and concomitantly decreases the probability for excitons to be trapped at these centres, resulting in a strong enhancement of the PL intensity. The increase in the PL efficiency reaches two orders of magnitude for the sample grown at 410 K relative to the one grown at 230 K [26]. Thus the increase of the PL efficiency accompanied by the red shift of the PL band determines the increase in the background of the Raman spectra of the films grown at elevated substrate temperatures.

3.2. PTCDA/S-GaAs(100)

The PTCDA samples produced on S-GaAs(100) substrates had similar colours to those on Si(100) substrates. At evaporation rate of ~ 0.3 nm/min the growth only takes place for a temperature below 470 K. As in the case of Si(100) substrates a granular structure can be observed. AFM topographic images (shown in [28]) reveal islands with an average lateral size of about ~ 70-80 nm in the films grown at RT. At higher temperatures of growth, larger island sizes are achieved (~ 400 nm at 360 K and ~ 1000 nm at 410 K). When grown at 360 K and above the grains have well defined edges that are parallel to one of the substrate main axes ([011] or [0$\underline{1}$1]) [28].

The Raman spectra of PTCDA samples on S-GaAs(100) again show the increasing background in the low frequency range which is related to the increase in the island size [28]. On the other hand, the background in the high frequency region shows that the PL has a maximum efficiency for the sample grown at 360 K. This can be explained by a critical value of the grain surface to volume ratio that dictates the number of non-radiative centres in the film [28]. However, both the roughness- and PL-related backgrounds are larger for the samples grown on GaAs substrates compared to those grown on Si at the same temperatures [7].

The line-shape of the C-H deformation mode at 1303 cm^{-1} changes very little as a function of substrate temperature of growth. This proves that the S-GaAs(100) substrates favour the formation of β-phase also at elevated temperatures, contrary to Si(100) [28]. Thus the increase in grain size with increasing substrate temperature during growth appears to be a characteristic for the passivated H-Si(100) and S-GaAs(100) substrates (this work) as well as for Si(100) substrates covered by natural oxide [29] and for NaCl(100), KCl(100) and quartz [27]. This effect is accompanied by the increase in α/β ratio for H-Si(100), NaCl(100), KCl(100) and quartz [27] substrates and by the decrease in α/β ratio for S-GaAs(100) substrates.

3.3. DiMe-PTCDI/S-GaAs(100)

3.3.1 SEM

The DiMe-PTCDI films grown onto S-GaAs(100) substrates reveal also an island structure when investigated by means of SEM (Fig. 3). In films grown at RT with thicknesses of 40 nm (Fig. 3(a)) most of the grains have a circular shape with an average lateral size of 80 nm to 100 nm. In thinner films (up to 20 nm) the majority of the grains are ribbon-like, with the ribbon axes making an average azimuthal angle of ~ ±10° with the [011] axis of S-GaAs(100) [30].

To investigate the influence of the substrate temperature of growth on the film morphology DiMe-PTCDI deposition was preformed at RT and 360 K. The films grown at elevated temperatures (360 K) consist predominantly of ribbon-like grains with a width of ~ 100 nm to 200 nm and length above 500 nm (Fig. 3(b)). These grains are preferentially oriented with their long edge parallel to the [011] axes of the substrate and are separated by voids of the order of 100 nm. This confirms again the trend observed for PTCDA grown on different substrates that the elevated substrate temperatures favour the formation of spatially extended domains.

3.3.2. Raman spectroscopy

The signal obtained with the XRD laboratory facility for the DiMe-PTCDI films was insufficient to draw any conclusion regarding the crystalline nature of the domains observed by SEM. In such a case the presence of external molecular phonons in the Raman spectra may be of great help for the demonstration of the crystalline nature of films. The overview Raman spectra of films having ~ 40 nm nominal thickness deposited onto substrates kept at RT and 360 K are shown in Fig. 4. The spectra were normalized with respect to the C-H mode at 1290 cm^{-1} and the low frequency region was enlarged by a factor of 5.5.

The number and frequency positions of phonons detected in films grown at both temperatures considered in this work correspond to those detected in a single crystal for which the XRD measurements proved a crystalline composition with monoclinic symmetry. Recalling the islanded structure evidenced by SEM it can be concluded that the films are polycrystalline. It must be mentioned that a remarkably strong polarization response for external as well as for internal modes was observed for both films. Considering that the spot size for the *in situ* experiments allows more than 10^5 grains with various sizes to be probed, it can be concluded that all crystalline domains have a preferential orientation with respect to the substrate.

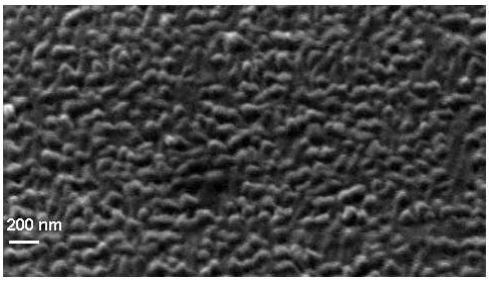

a

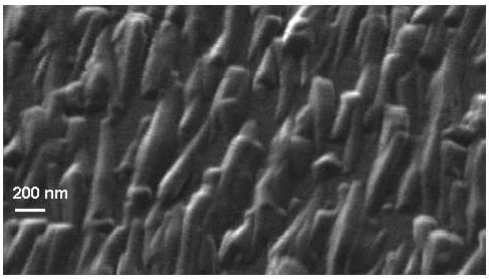

b

Fig. 3. SEM images of 40 nm DiMe-PTCDI films grown onto S-GaAs (100) substrates maintained at RT (a) and 360 K (b).

As in the case of PTCDA the roughness-related background affecting the spectra below 125 cm^{-1} increases in the film grown on the substrate at elevated temperatures, reflecting the increase in size of the crystalline domains. The narrowing of phonon bands is also observed, reflecting the increasing grain size and the reduction in number of intrinsic defects.

The effect of growth conditions on the internal modes with C-H deformation character (Fig. 4, inset) resides in changing the relative intensities. The ratio between the intensities of the mode at 1301 cm^{-1} and 1290 cm^{-1} increases with the film thickness in the unpolarized spectra when the growth takes place at RT. This ratio was also found to be larger in parallel compared to crossed polarization, due to the lower symmetry of the mode at 1290 cm^{-1} which has large contribution from CH_3 vibrations.

The mode at 1301 cm^{-1} originates from C-H deformations involving H atoms susceptible to be participate in H bridges (see the elongation patterns in Fig. 4). Thus its intensity can be lowered by the presence of molecules located at substrate interfaces or grain boundaries as well as by the presence of intrinsic defects. The ratio observed in the unpolarized spectra of the 40 nm film grown at 360 K is larger compared to that in the RT film, as a result of larger grain size and probably, improved crystallinity.

3.3.3. Infrared spectroscopy

Infrared measurements on PTCDA/S-GaAs(100) samples reveal isotropy in the substrate plane. The ratio of the in-plane molecular modes with respect to the out-of-plane ones is similar to that observed for PTCDA/Si(111). Quantitative analysis of this ratio reveals that the molecular planes of the PTCDA molecules form an average angle of ~9° with respect to the Si(111) substrate plane [31].

The results of infrared measurements for 120 nm DiMe-PTCDI on S-GaAs(100) are given in Fig. 5 for the region of the C=O modes. The mode at 1657 cm^{-1} is characterized by a dipole moment along the short molecular axis and will therefore be labelled as *y* mode while the mode at 1693 cm^{-1} originates from a molecular vibration along the long molecular axis and is therefore labelled as *x* mode.

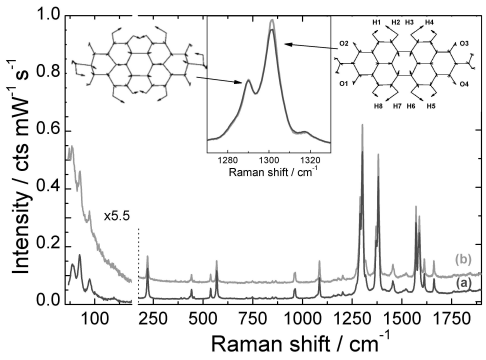

Fig. 4. Raman spectra of DiMe-PTCDI films grown onto S-GaAs(100) at two substrate temperatures: 295 K (a) and 360 K (b). Inset shows a zoom in the region of C-H modes.

The spectra were recorded in reflection with s-polarised light at near normal incidence under azimuthal rotation. The azimuthal angle γ describes the angle between the plane of incidence and the [011] direction of the substrate. For example at γ = 0° the plane of incidence contains the [011] direction of the substrate and the electric field vector is parallel to the [0-11] GaAs direction.

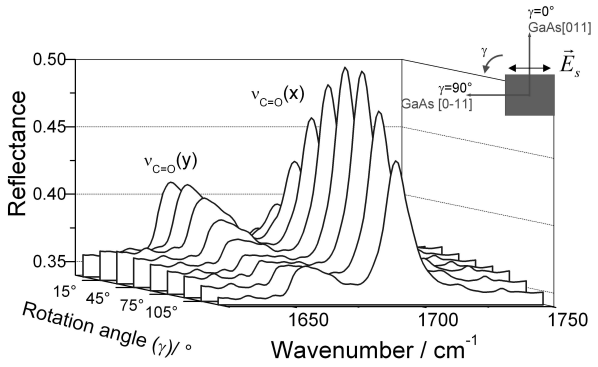

Fig. 5. Infrared spectra of a 120 nm DiMe-PTCDI film recorded upon azimuthal rotation.

The intensity of the modes varies with the azimuthal angle and maxima of *z* (not shown) and *y* modes are shifted by an angle of about 90° with respect to those of the *x* modes. Maxima are observed at angles $\gamma_{max}(y) = 7°$ and $\gamma_{max}(x) = 94°$. That means that the intensity of the x mode is maximal when the electric field vector makes an angle 184° and with the [011] GaAs axis. This indicates a preferential orientation of the molecules with their long axis close to parallel to the [011] axis of the GaAs substrate. A more detailed analysis of infrared spectra for the determination of the molecular orientation can be found in ref. [30].

4. Summary

In this contribution a variety of techniques was employed to asses the morphology and structure of thin films of PTCDA/H-Si(100), PTCDA/S-GaAs(100) and DiMe-PTCDI/S-GaAs(100) were investigated as a function of the substrate temperature during film growth in the temperature range 230 K to 410 K.

SEM and AFM studies showed that all the films consist of islands. The crystalline nature of the PTCDA and DiMe-PTCDI films was evidenced by the observation of external molecular phonons in the Raman spectra. The decrease in the FWHM of molecular phonon bands observed with increasing substrate temperature during growth can be related to an increase in the size of the crystalline domains and improvement of crystallinity. This increase in the size of the crystalline domains was independently confirmed by the AFM and SEM results.

The PTCDA films consist of a mixture of two polymorphs α and β having the same symmetry and very similar lattice parameters. The silicon substrates kept at elevated temperatures favour the growth of α- at the expense of the β-phase, while the situation is reversed in the case of GaAs substrates. A preferential orientation of the DiMe-PTCDI molecules with their long molecular axis close to parallel to the [011] axis of the GaAs substrate was evidenced by the infrared spectroscopy results.

Acknowledgement

The authors acknowledge the EU funded Human Potential Research Training Network DIODE (Contract No.: HPRN-CT-1999-00164) for financial support.

References

[1] W. Kowalsky, DFG-Abschlußbericht Ko 1040/7-1, TU Braunschweig, Institut für Hochfrequenztechnik (1998).
[2] D. R. T. Zahn, S. Park, T. U. Kampen, Vacuum **67**, 101 (2002).
[3] Y. Hirose, S. R. Forrest, A. Kahn, Phys. Rev. B **52**, 14040 (1995).
[4] C. Kendrick, A. Kahn, Appl. Surf. Sci. **123-124**, 405 (1998).
[5] C. Kendrick, A. Kahn, Surf. Rev. Lett. **5**, 289 (1998).
[6] Y. Hirose, S. R. Forrest, A. Kahn, Phys. Rev. B **52,** 14040 (1995).
[7] T. U. Kampen, G. Salvan, D. Tenne, D. R. T. Zahn, Appl. Surf. Sci. **175-176**, 326 (2001).
[8] N. Nicoara, I. Cerrillo, D. Xuaming, J. M. García, B. García, C. Gómez-Navarro, J. Méndez and A.M. Baró, Nanotechnology **13,** 352 (2002).
[9] A. Das, G. Salvan, T. U. Kampen, W. Hoyer, D. R. T. Zahn, Appl. Surf. Sci. **212-213**, 433 (2003).
[10] M. Möbus, N. Karl, T. Kobayashi, J. Cryst. Growth **116,** 495 (1992).
[11] A. J. Lovinger, S. R. Forrest, M. L.Kaplan, P. H. Schmidt, T. Venkatesan, J. Appl. Phys. **55**, 476 (1984).
[12] S.R. Forrest, Chem. Rev. **97**, 1793 (1997).
[13] E. Hädicke, F. Graser, Acta Cryst. C **42**,189 (1986).
[14] Z. Q. Gao, W. Y. Lai, T. C. Wong, C. S. Lee, I. Bello, S. T. Lee, Appl. Phys. Lett. **74**, 3269 (1999).
[15] D. S. Qin, D. C. Li, Y. Wang, J. D. Zhang, Z. Y. Xie, G. Wang, L. X. Wang, D. H. Yan, Appl. Phys. Lett. **78**, 437 (2001).
[16] C. González, I. Benito, J. Ortega, L. Jurczyszyn, J. M. Blanco, R. Pérez, F. Flores, T. U. Kampen, D. R. T. Zahn, W. Braun, Phys. Rev. B, submitted.
[17] T. U. Kampen D. R. T. Zahn, W. Braun, C. Gonzalez, I. Benito, J. Ortega, L. Jurczyszyn, J. M. Blanco, R. Perez, F. Flores, Appl. Surf. Sci. **212-213**, 850 (2003).
[18] I. De Wolf, J. Jimenez, J. P. Landesman, C. Frigeri, P. Braun, E. Da Silva, E. Calvet, „Raman and Luminescence for Microelectronics“, Catalogue of optical and physical parameters, published by the European Commission, Directorate General Science,

Research and Development (1998).
[19] T. Ogawa, K. Kuwamoto, S. Isoda, T. Kobayashi, N. Karl, Acta Cryst. B **55**, 123 (1999).
[20] G. Salvan, D. Tenne, A. Das, T. U. Kampen, D. R. T. Zahn, Org. Electronics **1**, 49 (2000).
[21] P. S. Pizani, F. Laniotti, R. G. Jasinevicius, J. G. Duduch, A. J. V. Porto, J. Appl. Phys. **87**, 1280 (2000).
[22] M. A. Paesler, D. E. Sayers, R. Tsu, J. Gonzales-Hernandez, Phys. Rev. B, **28**, 4550 (1982).
[23] G. Salvan, D. R. T. Zahn, Europhys. Lett. **67**(5), 827 (2004).
[24] E. V. Tsiper, Z. G. Soos, Phys. Rev. B **64**, 195124 (2001).
[25] A. Kytoivi, S. Haukka, J. Phys. Chem. B **101**, 10365 (1997).
[26] G. Salvan, C. Himcinschi, A. Yu. Kobitski, M. Friedrich, H. P. Wagner, T. U. Kampen, D. R. T. Zahn, Appl. Surf. Sci. **175-176**, 363 (2001).
[27] M. Leonardth, O. Mager, H. Port, Chem. Phys. Lett. 313, 24 (1999).
[28] G. Salvan, S. Silaghi, B. Paez, T. U. Kampen, D. R. T. Zahn, Synth. Metals **154**, 165 (2005).
[29] M. Möbus, N. Karl, Thin Solid Films **215**, 213 (1992).
[30] M. Friedrich, G. Gavrila, C. Himcinschi, T. U. Kampen, A. Yu. Kobitski, H. Méndez, G. Salvan, I. Cerrilló, J. Méndez, N. Nicoara, A. M. Baró, D. R. T. Zahn, J. Phys.: Condens. Matter **15,** S2699 (2003).
[31] R. Scholz, M. Friedrich, G. Salvan, T. U. Kampen, D. R. T. Zahn, J. Phys. Cond. Matter **15**(38), S2647 (2003).

* Corresponding author: salvan@physik.tu-chemnitz.de